Referee Comments #1 (acp-2017-942-RC1-supplement) and author response.
Simone M. Pieber et al.

We thank the editor and referees for their comments. To guide the review process we have copied the referee comments in black text. Our responses are in regular blue font. We have responded to all the referee comments and made alterations to our paper (*in italic text*) and removed redundancies for clarification. Along with the revision we suggest a slightly changed title: "*Gas phase composition and secondary organic aerosol formation from gasoline direct injection vehicles with prototype particle filters investigated in a batch and flow reactor*"

General:

RC1: Interactive comment on "Gas phase composition and secondary organic aerosol formation from gasoline direct injection vehicles investigated in a batch and flow reactor: effects of prototype gasoline particle filters." By Simone M. Pieber et al

This paper evaluates the gas phase composition and secondary organic formation from gasoline vehicles in a batch and flow reactor. Excusive results about primary emission factors, gas vapor composition and SOA formation are shown. This paper is well written and organized. The paper describes a large amount of data, but critical evaluation and analysis is missing, that is needed to have confidence on the quantification of results. Therefore I recommend that the paper may be published in ACP after addressing the major revisions below.

Author Response: We agree with referee 1 that our manuscript describes an extensive data set on GDI vehicles with novel after-treatment systems, including a comprehensive analysis of the gas- and particle phase, as well as the SOA formation. We are confident, that our manuscript at its initial stage includes an extended discussion of experimental uncertainties in the main text and provides additional critical evaluation in detail in main text and supporting information. We provide answers to RC1 and modifications to our manuscript to the best of our abilities.

Major revisions:

RC1-1: 1) The analysis of vapor losses to walls is inadequate. Enormous progress has been made on this area recently, and there is no excuse to ignore those corrections in current studies. Comparability with past studies that were performed when vapor wall losses were not understood is not an excuse to ignore this major issue. Comparability with future studies, for which all the good ones will include analysis of this effect, should be the relevant criterion. It will benefit the citation of this paper for showing both results. This is an essential correction which could introduce large bias (a factor of 3-4 in Zhang et al. 2014) and is related to multiple key calculation including SOA yield, NMHC composition etc. Taken vapor loss corrections into account, comparison results can be more accurately assessed, especially crucial for some main focuses of this paper: SOA yield between SC and OFR, SOA yield of vehicle exhaust vs single precursors. As the authors stated in page 21 line 27-29 "we expect both SC and OFR yields to be underestimated, by factors of approximately 1.5-2 (SC) and 1.25 (OFR) ((Platt et al., 2017);(Zhang et al., 2014);(Palm et al., 2016)) due to vapor wall losses. Corrections would reduce the discrepancy between the two systems." Thus a gas vapor wall loss correction is needed for this study. The model of Krechmer et al. (2016) can be used for the SC, and has been recently shown ((Ye et al., 2016); also at AAAR 2017) to be consistent among all Teflon chambers. The model of Palm et al. (2016) should be applied to the OFR.

Author Response: We agree with the need to address vapor wall losses in smog chamber (SC) and oxidation flow reactor (OFR) studies. For this reason, we have provided estimates for vapor wall losses for both systems in the initial version of the manuscript, as the referee mentions in the second part of this comment. We believe that our transparent approach to provide the data along with the expected correction factor which we have determined for this specific smog chamber, using gasoline vehicle emissions in our related publication (please refer to Platt et al., 2017), is a valid option, as dedicated experiments to study the exact losses during the presented experiments have been missing. It would be misleading to apply correction factors from literature. We would like to note, that the correction factor determined in Platt et al., 2017 (1.5-2) is in line with reports by others (e.g. Zhang et al., 2014, reports a factor of 1.1-4.2 underestimation, La et al., 2016, found a factor of 1.1.-6). Generally, we disagree that gas/vapor loss corrections are transferrable from one chamber to the next

without specific characterization experiments, and don't see this as a conclusion in previous literature reports either (see Krechmer et al., 2016).

Regarding the OFR, the model from Palm et al., 2016, has been applied in the initial version of our manuscript and the corresponding correction factor is already stated in the manuscript.

Loss corrections on our primary NMOC composition are not needed: The compounds of interest for SOA formation which we were able to identify by PTR-ToF-MS in our emissions mix are mainly BTEX, C3-Benzenes and Naphthalene. Based on their saturation mass concentration, these compounds are classified as VOCs or correspond to the upper end of the IVOC range, and are therefore not expected to be impacted significantly by losses to SC walls on a time-scale relevant to our SOA study. We performed measurements with emissions containing these substances to test their loss to chamber walls without oxidation chemistry initiated, and have monitored the aromatic composition and absolute concentrations of our identified species over the course of several hours: it did not change significantly enough to impact our findings, i.e. during experiments lasting between 2 and 6-8 hours the stability of relative gas phase composition (determined as the change in the ratio of relevant SOA-precursors to benzene) changed only by 3% (after 2 hours, which is a typical time-scale for the presented experiments) to 7-12% (at 6-8 hours).

Text modifications: We have modified the section (2.2.5) to include also additional references to newer literature and report the possible spread for SOA yield underestimations better. The new text reads as follows:

- *"a robust strategy for their determination and correction remains challenging (Krechmer et al., 2016). In our previous work, we estimated that vapor wall losses may cause SOA yields to be underestimated for the SC used herein (assessed based on gasoline vehicle exhaust SOA, see Platt et al., 2017, by a factor 1.5-2 for our experimental conditions), comparable to suggestions by others, e.g. a factor of 1.1.-4.2 by (Zhang et al., 2014) and 1.1-6 (La et al., 2016). Data correction would increase SOA yields on average by a factor 1.5-2."*
- *"Given the high SOA concentration and hence particle surface ((1-5)x10^{9} nm^{2} cm^{-3} based on the SMPS size distribution of SOA), at least 80% of the formed LVOC was calculated to partition to the pre-existing OA mass based on the model by Palm et al., 2016. Data correction would increase SOA yields by a factor of 1.25 on average."*

RC1-2: 2) The comparison on SOA formation between OFR and SC should also consider gas vapor loss in the tubing (Pagonis et al., 2017). The different tubing lengths and materials can also result in a SOA yield difference between SC and OFR. A vapor loss calculator can be found in Pagonis et al. (2017). Please clarify the tubing material and length as well. Page 16 line 17-18: In addition to the residence time of OFR, this SOA delay was also possibly caused by the delayed gas vapor in the tube, as suggested in Pagonis et al. (2017).

Author Response: We agree that this should be specified.

Tubing material and length: Tubing to sample direct emissions from the vehicle tailpipe for a) injection into the SC or online-OFR, or b) direct gas-phase measurements are made of SilcoTek®-coated steel (12 mm diameter), temperature controlled at 140°C, operated under high flows (30 L min^{-1}), and of roughly 8 m length. Ejector dilutor 1 is placed in a temperature controlled housing (200°C), and ejector dilutor 1 is operated at 80°C. Instruments sampling either a) from the SC or b) behind the OFR, or c) directly, are connected via separated tubing for gas-phase and particle phase. Particle-phase tubing is exclusively made of stainless steel, no copper tubing is used. Sampling lines are of 6 mm diameter, and up to 2 m length. Support pumps are used at the instrument inlets, to minimize sampling residence time by increasing the flow rate. Similar approach is used for gas-phase sampling (total tubing length to reach all of the instrument inlets, which are also equipped with support pumps is up to 2 m). Tubing for gas-phase sampling is made of either SilcoTek®-coated steel or Teflon, temperature controlled at 60°C where necessary (i.e. for PTR-ToF-MS measurements and FID), to avoid losses of the VOC and IVOC species relevant to our SOA-study and PTR-ToF-MS analysis (including essentially BTEX, C3-Benzenes, Naphthalenes, and eventually phenolic compounds, benzaldehyde). SilcoTek®-coating and Teflon are also suitable for the sampling of species known to be easily retained on surfaces, such as formaldehyde, acetic acid, acetaldehyde, for which, in addition to the uncertainties of PTR-ToF-MS analysis, also tubing losses may induce a slight shift in our gas-composition analysis.

We are confident that the differences in SOA yields obtained in the SC and OFR are not caused by losses on sampling lines between the SC and OFR. This sampling system was made of a combination of SilcoTec® coated steel with carbon-coated Teflon (i.e. electrically conductive Teflon suitable for simultaneous gas- and particle phase sampling), and the total length between SC and OFR inlet was roughly 35 cm (6 mm diameter, ca. 8 L min^{-1} flow). Additionally, all measurements from the dark smog chamber (which is the basis for gas-phase composition data), were performed for at least 10-15 minutes, to reach a stable signal. We experimentally determined potential losses in the sampling from dark smog chamber and sampling through dark OFR and observed a reduced mass of species by less than 5% and no change in the composition of the SOA precursors, which, in our case, is the determining factor.

Page 16, Line 17-18: Our statement is in line with findings of other researcher (Zhao et al., 2018), who state "After the vehicle was turned off at the end of bags 2 and 3 it took approximately 3 min for the OA signal at the PAM reactor outlet to return to background levels. This delay reflects the time it takes for the exhaust to pass through the PAM reactor.", in analogy to our interpretation. However, we do generally agree that delays due to retention on sampling lines can cause a shift in the signal, and hence add this also specifically to our manuscript.

Text modifications: Tubing material, length, temperature and flow rates are specified in the SI as follows:

- *Tubing to sample direct emissions from the vehicle tailpipe for injection into the SC or online-OFR, or direct gas-phase measurements are made of SilcoTek®-coated steel (12 mm diameter), temperature controlled at 140°C and operated under high flows (30 L min^{-1}) to avoid substantial losses over the sampling length of roughly 8 m. Ejector dilutor 1 is placed in a temperature controlled housing (200°C), and ejector dilutor 1 is operated at 80°C.*
- *Instruments sampling either from the SC, behind the OFR, or directly from the dilution system are connected via specific tubing for gas-phase and particle phase. Particle-phase tubing is made of stainless steel (6 mm diameter), and up to 2 m length. Support pumps are used at the instrument inlets, to minimize sampling residence time by increasing the flow rate. Total tubing length to reach all of the gas-phase instrument inlets, which are likewise equipped with support pumps is up to 2 m. Tubing is made of Teflon or SilcoTek®-coated steel. The sampling line of the PTR-ToF-MS instrument and FID is temperature controlled at 60°C.*
- *SilcoTek®-coating and Teflon are also suitable for the sampling of species known to be easily retained on surfaces, such as formaldehyde, acetic acid, acetaldehyde, for which, in addition to the uncertainties of PTR-ToF-MS analysis, also tubing losses may induce a slight shift in our gas-composition analysis.*
- *The sampling system between the SC and OFR (for OFR-from-SC experiments) was made of a combination of SilcoTec® coated steel and conductive Teflon tubing, suitable for simultaneous gas- and particle phase sampling. The total length between SC and OFR inlet was roughly 35 cm (6 mm diameter, ca. 8 L min^{-1} flow). Additionally, all measurements from the dark SC batch sample were performed for at least 10 minutes, to reach a stable signal."*

Signal delay was adressed as follows:

***"**The latter is related to a delay of the OFR signal by the residence time in the reactor, as also observed by others (Zhao et al., 2018), and might potentially also be caused by a delay of SOA forming species which are retained on surfaces (Pagonis et al., 2017)."*

RC1-3: 3) The particle losses due to heating in the sampling line and the hotter temperature in SC when UV light is on should be addressed. The aerosol loss due to tubing (under no heating condition) needs to be estimated as well. The model for aerosol loss calculation in the tubing can be found in (von der Weiden et al., 2009). The particle loss due to heating can be experimentally determined.

Author Response: Particle losses in the SC are assessed with our data as presented in our initial manuscript, which takes all factors leading to particle losses, including temperature effects into account.

Text modifications: "The main losses of particles are due to (1) diffusion, (2) electrostatic deposition and (3) gravitational settling, *which are in turn affected by temperature changes due to the UV lights.* Wall losses of particles in the SC were accounted for using the method described in (Weitkamp et al.,

2007) and (Hildebrandt et al., 2009), *which accounts for all these loss processes simultaneously, including the aforementioned temperature effects*."

RC1-4: 4) Page 10 line 20-30: The SOA photolysis in OFR should be considered as well. For example in OFR with full UV light setting (100%), half of the SOA from toluene SOA (OH chemistry) or naphthalene SOA (OH chemistry) can be photolyzed under 254 UV light with a low quantum yield of 0.1, as shown in Fig. 8b in (Peng et al., 2016). This photolysis effect on SOA formation and SOA yield calculation under 50% and 100% UV light setting should be considered.

Author Response: Non-OH losses of SOA precursors via photolysis within the OFR was assessed for all our experimental conditions (OFR-from-SC, online-OFR 2014 and online-OFR 2015) as described in the discussion manuscript (section 2.2.5 and the corresponding information in the SI).

We summarize our findings and implications here: Given that non-OH losses strictly only imply a non-OH induced reaction of the compounds, but do not rule out any SOA formation from the obtained reaction/photolysis products, no corrections for any non-OH reaction can be made in our view (as already stated in our manuscript) regarding the formation of SOA. However, we agree to note specifically that the observed SOA may not only be related to OH-induced aging but also to UV-induced reactions that produce SOA, (in addition to potential O_3-induced SOA, as well as NO_3-induced SOA). Our discussion paper contains this information already in the SI (page 3, line 5) as follows *"This only refers to the reactive interaction of OH vs. the excitation by UV, and does not allow conclusions on the formation of SOA. Also chemistry initiated by UV185 or UV254 may lead to the formation of SOA. Additionally, it does not suggest any conclusions about the interaction of O3 with double bonds made available by first ring-opening reactions." (…) "Potential effects of O3 on first generation products are not taken into account. Under those diluted conditions (initial NO < 100 ppb), we regard the experiments in OFR as low NO conditions (Peng and Jimenez, 2017). The dominant SOA precursors found in the exhaust are not reactive towards NO3 radicals that can be formed in the OFR; potential effects on first generation products are not taken into account."*

In this specific comment (RC1-4), the referee addresses in addition the destruction of previously formed SOA by photolysis, which we have not previously addressed in our manuscript. We address this here: Our OFR photon-flux is $(1.2\text{-}2.3)\times10^{15}$ photons cm^{-2} at 185 nm and $(1.7\text{-}2.9)\times10^{17}$ photons cm^{-2} at 254 nm (100% UV setting, which is the maximum and hence inducing maximum photolysis impact). Those photon-fluxes can be considered "medium" if comparing to Peng et al., 2016, Figure 8. The estimated SOA-photolysis is <1% for naphthalene at a quantum yield of 0.1 and <5% at a quantum yield of 1, for 185 nm. For 254 nm, the estimated SOA-photolysis is around 20% at a quantum yield of 0.1, but reaches 60-80% if a quantum yield of 1 is assumed, according to Figure 8 in Peng et al., 2016. Significant uncertainties are associated with this assessment: 1) we do not have any precise information about photon fluxes of our OFR, 2) dependent on the assumption of the quantum yield, we obtain a result which ranges from insignificant to significant, 3) as a full description of the chemical composition of the SOA is missing, it is not clear which effects photon-interactions will induce and whether photolytic destruction of molecules will lead to a loss of SOA mass and to which extent; hence, this assessment is at the current point in time of speculative nature only. Future work should address this in further detail before any corrections can be applied. Our conclusion is in line with Peng et al., 2016, who state: "Thus, to our current knowledge, lack of solid information on quantum yields of SOA components with multiple carbonyls and hydroxyls at 254nm prevents a clear assessment of SOA photolysis in OFRs at the medium and high UV.

Text modifications: *"… Also chemistry initiated by UV185 or UV254 may lead to the formation of SOA, and likewise photons may also lead to the destruction of OH-formed SOA; both processes deserve attention in future research."* was added to the corresponding SI section, and "*The results and implications of photon-induced effects on SOA formation or destruction are discussed in the SI.*" was added to the main text.

RC1-5: 5) Page 14 line 1-2. How did the mass quantification between AMS and SMPS compare? It is essential to document this comparison in the form of scatterplots and regressions. Collection efficiency (CE) vary with chemical composition and aerosol phase (Middlebrook et al., 2012). CE for AMS quantification should vary in this study since relative OA and NO3 fraction in total aerosol changed a lot. Why do the authors choose a CE ~1 here. I would expect a slight variation on RIE

since there were POA dominated periods during the studies, for which RIE may be higher (Jimenez et al., 2016; Murphy, 2016). Attention needs to be paid for the size cut differences between AMS and SMPS as well, when nucleation was happened.

Author Response: CE: Typical assumptions for ambient aerosols assume CE=0.5, which is related to large extents to the fact that ambient aerosol contains ammonium sulfate and solid or glassy organics, which lead to significant bounce on the AMS vaporizer. Ammonium-Nitrate and Organic Aerosol mixtures are not expected to bounce significantly, and hence we have used a CE=1. Middlebrook et al., 2012, observed a CE close to 1 (0.8) for ambient aerosol containing ammonium nitrate, but no ammonium sulfate.

RIE: In principle, the RIEs of organic material may vary with the molecular weight of the parent molecule. However, most compounds undergo extensive thermal decomposition in the AMS and ionize as much smaller molecules, which have similar ionization cross-sections and thus similar RIEs. In the current study, the observed POA is dominated by aliphatic hydrocarbons, which have been shown in other studies to have RIEs of approximately 1.4, the same as SOA (Jimenez et al., 2016). For example, there is no significant difference in the decane, diesel fuel, and lubricating oil despite a factor of 2 differences in molecular weight. Therefore we do not expect significant differences between POA and SOA RIEs in this study. Further, even if the POA and SOA RIEs were different, the very low POA/SOA ratios observed in this study would prevent a significant bias in the results, even if the POA RIE was as high as that suggested by Murphy et al., 2016 (~4 assuming the molecular weight of lubricating oil), which we note again would be in conflict with experimental evidence (Jimenez et al., 2016), our conclusions won't be affected. An RIE of 1.4 for SOA remains reasonable, and hence, any conclusions on SOA yields are neither effected by applying the standard assumption of RIE=1.4 to our data set.

Lens-cut-off/Nucleation: AMS pToF size distributions are described in the SI. As provided in the main text, no lens-transmission analysis was performed.

Text modifications: The new text reads as follows:

"We used a collection efficiency of 1, as upon photochemistry, significant amounts of NH_4NO_3 were formed, and under those $(NH_4)_2SO_4$ –free conditions, our aerosol mixture is not expected to bounce significantly. No corrections for lens transmission were performed, pTOF distributions are provided in Figure S10."

RC1-6: 6) Schematic of the sampling strategy is confusing. I did not get the timing for the sampling strategy. Was the UV light setting is constant during vehicle testing cycle? Then the background of aerosol and gases under UV light is off in SC and OFR was obtained by repeating the testing cycle of the cars? Sufficient detail needs to be provided, that would enable someone else to repeat the experiments, as it is standard in scientific publications.

Author Response: We have provided a lengthy (9 pages) description of our experimental set-up, strategy and conditions on Page 5-14 of the discussion paper (section 2 "Experimental"), which we believe allows for a full repeat of our experiments, specifically, this is true for our detailed description in section 2.2.1. Additionally, we refer to Platt et al., 2013 and 2017, in which we have published our experimental set-up earlier in further detail. Further, our photochemistry sampling scheme is discussed in section 3.5, along with representation of a typical experiment in Figure 5. We provide further information on background levels in our answer to RC2 and RC1-9 below, and have added additional information on control experiments to the text (see RC1-9). We have clarified this lengthy description to avoid confusions.

In the following our specific explanations:

- SC sampling: Background measurements were conducted prior each experiment and emissions were injected thereafter during a full cold-started test cycle or selected phases thereof. During this injection phase, emissions in the SC were only monitored with a limited set of experiments. The mass spectrometers for gas- and particle phase characterization were monitoring the direct emissions sampling (online) and online-OFR instead. When the cold-started emissions test was completed, mass spectrometers were set to characteriz the emissions sample collected in the SC for about 15 minutes; thereafter, the hot-started vehicle test was conducted for which instruments were again disconnected from the SC, to monitor

the online OFR and direct emissions instead. Meanwhile, no photochemistry was initiated in the SC.

- OFR-from-SC (also "batch-OFR)¨
  OFR-from-SC experiments refers to experiment that included aging a sample of emissions in the OFR reactor at fixed conditions, with UV lamps set to either 50, 70 or 100% intensity and with UV off (dark). Emissions which were pre-collected in the dark SC used as a buffer/storage volume were sampled via a short sampling system described in detail within answer to RC1-2 from the SC into the OFR. Sampling was conducted until the SOA formation in the OFR reached a stable signal, and conditions were kept stable for several minutes from this point onwards. Prior and after UV on conditions, fresh emissions (OFR UV off as well as directly in the SC) were characterized to allow for estimating the POA contribution to the OA mass measured under UV on conditions, as well as to allow for calculating the reacted SOA precursor mass. OFR cleaning with clean air under UV on conditions was performed prior to the measurements to minimize any background contamination.
- Direct emissions sampling (online): PTR-ToF-MS data were collected at the inlet of the OFR. These data were used for selected experiments (e.g. data on GDI4 in 2015, labelled "online"). For all other vehicles and experiments we present the average composition and emissions factors from samples that were collected in the SC (w/o photochemical aging). Essentially, integrating the direct emissions sampling (online) vs. the composition determined in the SC yielded comparable results (Figure 4, GDI4, SC vs. online).
- Online-OFR: yes, here we have tested vehicles up to 4 times with cold-started and 4 times with hot-started experiments (as stated in Table 1). Only one cold-started vehicle test could be conducted each day, hence, typically 3 cold-started vehicle tests were performed on 3 consecutive days with UV lights switched on in the OFR, and 3 hot-started vehicle tests with UV lights switched on. One a 4^{th} experiment day, we conducted the same set of experiment with OFR- UV lights switched off, to determine primary OA emissions and calculate the SOA. Essentially, much less POA was found then SOA (please see our online-OFR experiments, one of which is provided in the main text (Figure 3), as well as the corresponding figures in the SI). Note, however, that only for selected experiments (GDI4 in 2015), these online-OFR data were used in a quantitative way. For all other vehicles and experiments, we rely on SC and OFR-from-SC data (regarding SOA), as well as batch sampled experiments for primary NMOC composition. Essentially, integrating the online OFR-SOA for GDI 4 yielded comparable results to the SC (Figure 2b, GDI-4 SC vs. online).

Text modifications: We have made small modifications to shorten and clarified this section which has become more logic to facilitate experiment repeats now; information on backgrounds and control experiments was added as described in answer to RC1-9.

Other revisions:

RC1-7: Page 5 Line 8: EDC was defined as "older" low-road European Driving cycle (EDC), which is inconsistent with the definition of "New" EDC in the abbreviation/definition list.
Author Response: We have made the modifications to the abbreviations list, the modified text is provided in the following. The so-called "New European Driving Cycle", is by now the "older" cycle and overtaken by the recent "WLTC", which is, why nowadays, the NEDC is referred to as EDC, although the strict definition is "NEDC".
Text modifications: *"EDC =European Driving Cycle (previously known as the "New European Driving Cycle")"*

RC1-8: Page 7 line 26-27: Please specify the dilution factor for smog chamber (SC) and oxidation flow reactor (OFR).
Author Response: Dilution factors are provided in main text (Figure 1) and SI for our experimental set-up in the initial version of the manuscript. The final dilution value for the SC is determined by the volume sampled during a driving cycle. The decisive characteristic of a SC experiment are the concentration levels, rather than the dilution ratio, which are provided in Table S4-S7 of the initial SI.

Text modifications: Adjustments were made in section 2.2.2 and 2.2.3 to add the specific values for SC and OFR. "*Concentration-levels of our SC experiments were representative for urban ambient conditions, as reported in Table S4-S7."* and "*…the diluted exhaust (either 1 or 2 ejector dilutors, each at a dilution ratio of 1:8)…"*

RC1-9: Page 8 line 14-15: What is the aerosol background level in SC and OFR experiments with clean air when the UV light is on? If it is high, this background needs to be subtracted in the calculation of formed SOA mass concentration.

Author Response: The background was generally low (with UV off, as well as UV on, and the SOA background was insignificant compared to our typical experiments (<1 and <2 ug m^{-3} for SC and OFR respectively, during SC and OFR-from-SC experiments; < 10 ug m^{-3} during online OFR experiments (compared to 100 – 2000 ug m^{-3} SOA formed during these experiments, this is not significant). See also our response to RC-2. As we noted in the text, however, Ph2-4 experiments in the SC were close to the background measurements with the PTR-ToF-MS and hence we have noted this specifically in the discussion paper (figure caption of figure 4 "*Note that the total NMOC levels for Ph 2-4 (cW) are about 1/10 of full cW and Ph 1 (cW) concentrations only and measurements are close to the background measurements (signal not significantly different from 3 standard deviations of the background measurement"*).

Text modifications:

- *Background measurements of the clean chamber were conducted prior to each experiment, and was insignificant compared to our measurements except for Ph2-4 or GDI4 experiments as stated in the results. Photochemistry control experiments were conducted regularly to estimate the contribution of the SC background to SOA formation; these experiments were conducted after the standard cleaning procedure. Instead of vehicle exhaust, pure air was used as a sample and ammonium sulfate (50 ug m^{-3}) injected as seed. Other experimental procedures were in line with the typical vehicle experiments. We found a SOA background of < 1 µg m^{-3}, which is below the SOA concentrations formed during vehicle exhaust aging Concentration-levels of our SC experiments were representative for urban ambient conditions, as reported in Table S4-S7."*
- *"Background levels were <2 µg m^{-3} SOA before OFR-from-SC experiments (when sampling from cleaned SC) and <10 µg m^{-3} when sampling diluted (1:8) test bench room air prior online-experiments."*

RC1-10: Page 8 line 26-29: Figure S1 shows the aerosol and gas-phase species are sampled through the same tube in the center of OFR. If it is true, there will be large loss either on VOCs species (if stainless or copper tube is used) or on aerosols (if Teflon tube is used)

Author Response: We described our sampling system and tubing materials, length and flows in our response to RC1-major revisions, and have discussed implications for losses of the species of interest within our study in this response. We kindly ask the referee and editor to refer to this section.

Text modifications: As provided in "RC1-major revisions", we have added a description in the SI.

RC1-11: Page 9 line 26-27: The particle loss can be determined by measuring the aerosol concentration before and after OFR when the UV-light is off. The aerosol concentration before the OFR can also be roughly determined with aerosols in the SC chamber if the dilution factors and volatility of OA are known in OFR and SC. There have also been some reports from FIREX (Jesse Kroll's group) that particles containing BC can be charged by the UV lights and be lost much faster, also see (Federer et al., 1983). Was this effect evaluated?

Author Response: The referee refers to a sentence where we state that particle losses in the OFR were evaluated by comparing eBC concentrations before and after the OFR during experiments. We find this test to provide a more realistic evaluation of the OFR performance than the lights-off tests suggested by the referee due to differences in temperature and potential losses due to charging of BC particles by UV light, as suggested by the referee. As noted in the original manuscript, observed eBC losses were negligible, consistent with previous characterization of this OFR for similarly-sized particles (Lambe et al., 2011).

Although we have not specifically investigated the effects of UV charging, the fact that

overall BC losses are negligible across the OFR suggests that this loss process is also negligible for our experimental set-up.
Text modifications: No major adjustments were needed, we have modified wording to highlight that we are using an experimentally determined transmission under actual operating conditions ("in-situ"). The section reads now as follows: *"A comparison of eBC mass before and after the OFR indicated no significant losses during UV on or UV off periods (experimentally determined transmission was equal to 1).Consequently no further correction was applied. Particle wall losses in the OFR have been quantified previously by Lambe et al., 2011, who reported at least 80% transmission efficiency through the OFR for particles of mobility diameter (d_m) > 150 nm (Lambe et al., 2011). The particles measured behind the OFR in our study had a median vacuum aerodynamic diameter (d_{va}) between 200-400 nm based on HR-ToF-AMS measurements (size distributions are provided in Figure S9), which correspond to d_m > 150 nm when assuming spherical particles and an OA density of 1.2 g cm^{-3} (Turpin et al., 2001) supporting our experimentally determined transmission efficiency. "*

RC1-12: Page 10 line 16: "1000-5000 nm^2 cm^{-3}" Is this unit true? These values indicate the particle surface areas in this study are very small, which is inconsistent with mass values reported in Fig. 3. It is ~10^6 times less than those in the typical chamber studies, e.g. (Zhang et al., 2014).
Author Response: We thank the referee for spotting this typo. The values should indeed read (1-5)x10^9 nm^2 cm^{-3}. The particle surface area noted here corresponds to the OFR-from-SC aging experiments (i.e. an average SOA mass value of 100 µg m^{-3}), and no primary eBC seed (b/c of GPF installation) was present. We have revised the corresponding section to clarify this point further.
Text modifications: We have corrected the stated values to read (1-5)x10^9.

RC1-13: Page 11 line 19-24: Does the OH exposure estimated from BuOH-D9 agree with the OH exposure calculated based on Peng et al. (2015)? A plot showing the comparison of these two methods will beneficial for readers to understand how accurate of the OH exposure used here.
Author Response: The comparison requested by RC1 can be found in the SI of the current version of the discussion manuscript, as also highlighted in the main text. We copy-paste the information here:

"Based on these input parameters, the model (Peng et al., 2016) predicted an $[OH]_{exposure}$ (OH concentration integrated over time, see discussion in main text "OH exposure estimation", in molec cm^{-3} s) in the OFR of
UV100%: $[OH]_{exposure}$=(10-13)x10^{11}
UV70%: $[OH]_{exposure}$=(2.4-3.1)x10^{11}
UV50%: $[OH]_{exposure}$=(0.35-0.48)x10^{11}.
The estimated $[OH]_{exposure}$ (in molec cm^{-3} s) and OH concentration (in molec cm^{-3}), [OH], based on the experimental measurements of the decay of BuOH-D9 correspond instead to
UV100%: $[OH]_{exposure}$ =(3.0-5.8)x10^{11}, i.e. [OH]= (2.7-5.2)x10^9
UV70%: $[OH]_{exposure}$ =(1.6-2.5)x10^{11}, i.e. [OH]=(1.4-2.2)x10^9
UV50%: $[OH]_{exposure}$ =(0.31-0.49)x10^{11}, i.e. [OH]=(0.28-0.44)x10^9"

It appears that the model is able to re-produce our experimental measurements correctly at lower UV-intensity of the OFR reactor (i.e. the same order of magnitude is achieved), but fails to predict the OH exposure correctly at the higher UV intensity, where it over predicts the OH exposure). We believe the experimentally determined tracer-based method (d9-BuOH here) is more accurate because it is specific to the current system whereas the model is a generalized parametrization that here uses only the O_3-concentration as an input to determine the photon flux of the UV lamps. Therefore the tracer-based method is used throughout the manuscript and we strongly encourage other users of the OFR reactors to supply a proper tracer (such as BuOH-D9, see Barmet et al., 2012) for the experimental in-situ determination of the OH exposure whenever possible.

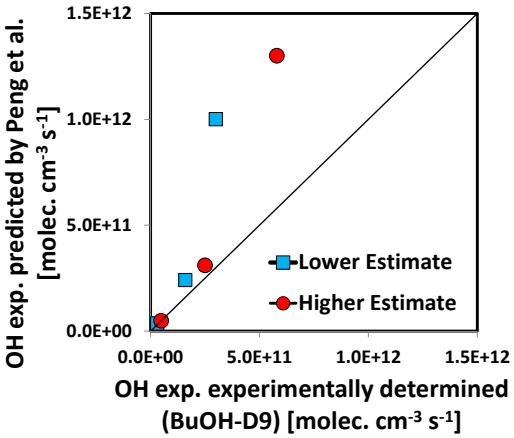

Figure R1-1. OH exposure predicted by the Peng-model vs. our experimentally determined OH exposure (data as stated in the SI). This plot was not added to the SI, as the data are compared in the text.

Text modifications: In the main text we have added the following: "T*he tracer-based OH exposure calculations are generally in good agreement with exposures predicted by the model, except at the highest OH exposures where the tracer method is approximately a factor of 2 higher. Tracer-based OH exposures are used throughout this analysis, as these measurements are specific to the current OFR system*."

RC1-14: Page 12 line 2: Please specify the dilution factor.
Author Response: The dilution ratio in the CVS-dilution tunnel is variable and was controlled by means of the CO2-analysis, and is at a range of 8 during high engines loads to 30-40 at idle conditions.
Text modifications: We added the information as described above.

RC1-15: Page 12 line 5-7: Why heat the sample before CPC? Why 300 oC.
Author Response: These settings are based on the PMP- Particle Measurement Program of the ECE GRPE Group; thermo-conditioning is a pre-requisite in order to measure only non-volatile particles.
Text modifications: We noted that we are not presenting any data from the CPC instrument in our manuscript and have therefore removed this statement from the main text, however.

RC1-16: Page 14 line 19-24: These descriptions cannot be found in the Fig. 1 e.g. No graph compares "Ph 1 of cW and hW vs. Ph 2-4 of cW and hW" in line 20.
Author Response: We are unable to follow the referee's argument. As we noted in the text, these comparison discuss the data presented in Figure 2, panel a and c. Specifically, the NMHC comparison for Ph 1 of cW and hW vs. Ph 2,3 and 4 of cW and hW are derived by looking at the data presented in Figure 2 panel c, and are discussed in the text.
Text modifications: No modifications were made specific to this request. However, we have revised Figure 2 along with suggestions by Referee 2 and have hence modified parts of section 3.1, which the Referee 1 refers to here; please refer to our response to RC-2.

RC1-17: Page 15 line 2-3: It is hard to draw such a conclusion based on Fig. 2b. A scatter plot between POA+BC vs PM is needed or at least please give the value POA+BC.
Author Response: We agree with the referee's argument, and have added a comparison plot in the SI to support our statement *"PM measured in the batch samples (sum of eBC and POA, Figure 2b) compares generally well with the gravimetric PM analysis of filters sampled from the CVS (Figure 2a)."*
Text modifications: As noted above, we have added an additional Figure to the SI and refer to it in the main text. *"PM measured in the batch samples (sum of eBC and POA) are compared with gravimetric PM analysis of filters sampled from the CVS in Figure S16."*

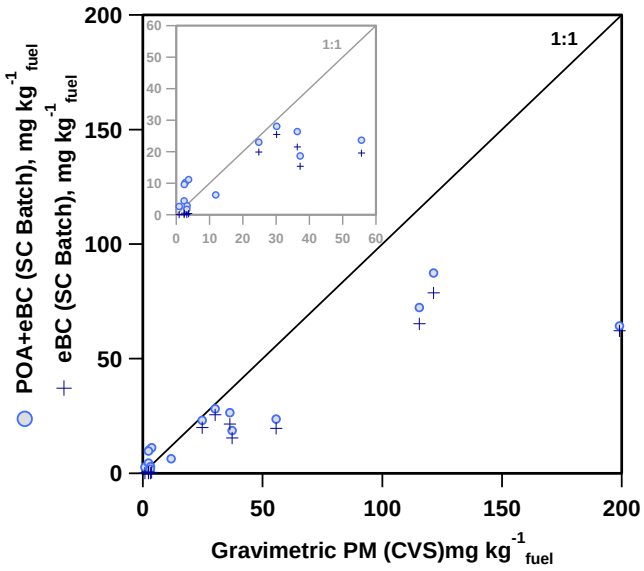

Figure R1-2: Comparison of POA+eBC from batch SC sampling to gravimetric PM measurements from filter samples taken from the CVS, added to the SI; the figure caption reads:
"POA and eBC measurements in the SC batch sample compared to gravimetric PM measurements from the CVS."

RC1-18: Page 15 line 9: Please give the value ranges for "previous finding".
Author Response: This information is provided in the current version of the discussion paper few lines further down ("*median 60, range ~10-400 mg kg^{-1} $_{fuel}$*"), i.e. on Page 15, line 12.
Text modifications: We have revised this paragraph to remove redundancies and make the range of previous findings easier to grasp for the reader, along with suggestion by RC-2.

RC1-19: Page 15 line 16-19: A smaller vapor loss in the OFR is also a possible explanation.
Author Response: We agree with the referee (as also indicated by our provided vapor correction factors 1.25 for the OFR and 1.5-2 for the SC) and have revised the statement.
Text modifications: As described above, we have put a reference to the subsections which discuss those issues at other locations within the manuscript.

RC1-20: Page 18 line 5: publishing year is required for "Jordan et al"
Author Response: Thanks for the hint; the reference was corrected.
Text modifications: "*Jordan et al.*" was revised to "*Jordan et al., 2011*".

RC1-21: Page 20 line 1: How to define the "high NO condition".
Author Response: The answer to the definitions is provided in the publication (Peng and Jimenez, 2017) which is cited along with above statement. We have clarified this now in our manuscript .
Text modifications: The statement *""high NO" conditions may be reached in the OFR ((Peng and Jimenez, 2017))."* was modified to read now *""high NO" conditions may be reached in the OFR as defined by (Peng and Jimenez, 2017)."*

RC1-22: Page 20 line 21: No OH exposure is shown in Fig. 6.
Author Response: We refer to the OH exposure data which are noted in the caption to Figure 6. We have clarified this statement.
Text modifications: The statement *"…OH exposure data at the end point of SC experiments and for the OFR are provided in Figure 6 and Figure 7)."* was revised and reads now *"OH exposure data at the end point of SC experiments and for the OFR are provided in caption to Figure 6, and Figure 7)."*

RC1-23: Page 21 line 5: Please clarify "Limited experimental statistics"
Author Response: We conducted 2 experiments with Ph2-4 emissions aged in the SC (1 with GDI1 with standard configuration and 1 with GDI1 equipped with a GPF). Additionally, Ph2-4 SOA-precursor emissions collected in the SC were close to background concentrations (as already discussed within this answer to referees as well as noted in caption to Figure 4). Therefore, the available data are not sufficient to allow a reliable SOA yield analysis for Ph2-4 analysis. Others (Zhao et al., 2018) have recently published a SOA yield comparison from an OFR data set on cold- and hot-engine emissions, and also discuss the potential background effects in their publication.
Text modifications: We have re-adjusted the main text, to read as follows: *"Data are presented as a function of suspended OA for all experimental conditions of cold-started GDI1-3 (i.e. for full cW, cE; and Ph 1 (cW)), while GDI4 or hot engine conditions, i.e. Ph 2-4 (cW) are not included in our the analysis, as this data set includes only two experiments with concentrations levels close to our background measurements; a discussion of SOA yields from cold- and hot-engine emissions has recently been published by Zhao et al., 2018 for an OFR data set)."*

RC1-24: Page 21 line 30-32: The fragmentation effect on aerosol phase under high OH exposure in OFR should also be considered.
Author Response: We are unable to follow the referee's argument. Page 21 line 30-32 discusses discrepancies among SC experiments, not OFR. Page 21 line 21 onwards discusses discrepancies between OFR and SC experiments, which, noting that they were conducted at somewhat different OA loadings, let us conclude that OFR-yields tend to be higher than SC yields, especially at higher OH exposures. Fragmentation (over functionalization) would tend to a) yield lower OFR SOA yields and b) as discussed in our previous publication (Bruns et al., 2015) and by Lambe et al., 2012, would yield higher O:C. We do not find any of these effects in our data set, hence, while we may be looking at compensating effects, we don't see results that seem to be driven into any direction by fragmentation only.
Text modifications: No modifications are required.

RC1-25: Page 22 line 12: "This generally indicates that we are able to identify the most relevant SOA precursors in the vehicle exhaust." This statement is not true. The SOA yield in SC and OFR was calculated based on a larger group of ArHC than merely OXYL/TOL. The author should calculated the SOA formation based on OXYL/TOL consumption in the SC (and OFR) and yield from OXYL/TOL experiment. Then compare the calculated SOA to the SOA formed in the SC.
Author Response: We agree with the referee's observation. We have used two different ways to approach the mass closure in our manuscript: 1) with a forward closure as presented in the initial Figure 5 as an example for 1 experiment (i.e. the reacted aromatic SOA precursor mass was weighted by a fixed SOA yield from the literature, which is the procedure suggested by the Referee 1 on RC1-25), and 2) via an indirect approach normalizing the formed SOA to the reacted ArHC mass (i.e. deriving an "effective yield" combining all reacted species), which allows to present the result as a function of OA loading. Because it appears confusing to have two different methods to address this, we decided to remove the SOA-closure from initial Figure 5 (bottom panels), and instead present data as "effective yield closure" (Figure 6) only.
Text modifications: We have revised all text sections to allow this modification; instead of a mass closure we discuss the results now in terms of a yield-closure in the original section 3.6. We have removed the statements on the mass closure from the text.

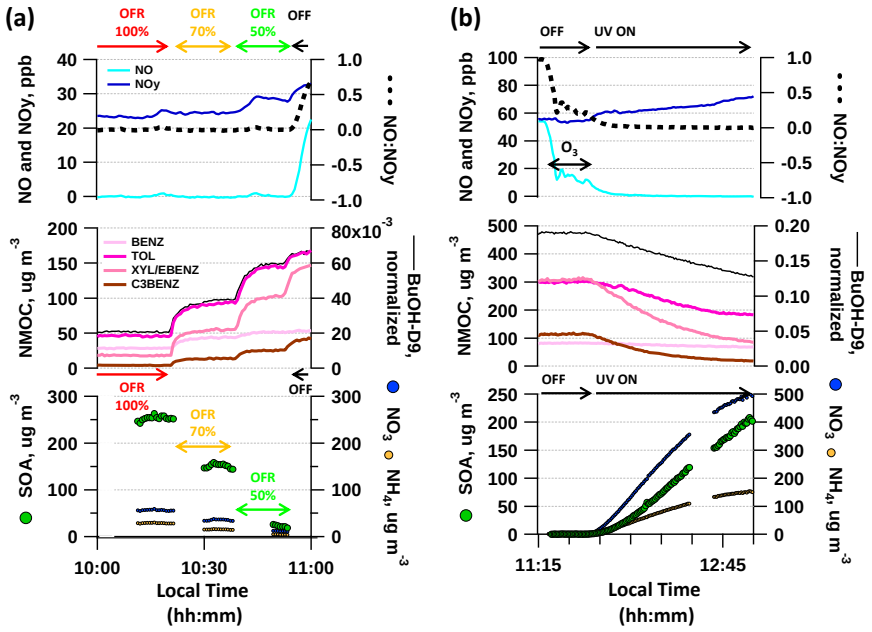

Figure R1-3: New Figure 5 with modified lower panels; the new figure caption reads as follows:
"Typical OFR-from-SC and SC photochemistry experiment. *Decay of dominant SOA precursors (benzene (BENZ), toluene (TOL), o-/m-/p-xylene (XYL) or ethylbenzene (EBENZ), C3-benzenes (C3BENZ)) upon photochemistry and associated SOA formation in* ***(a)*** *OFR (sampling from SC batch at different UV intensities, displayed is expt D3) and* ***(b)*** *SC (displayed is expt B1).* ***(a-b)*** *UV status and O_3 are indicated along with the NO:NO_y ratio and the OH tracer BuOH-D9. Reacted ArHC fractions are provided in the SI per experiment, see Figure S4. Local time is given in intervals of* ***(a)*** *30 min and* ***(b)*** *15 min."*

RC1-26: Page 24 line 13-14: To conclude this, it is better to plot a graph showing O:C comparison as a function of OH exposure between SC and OFR. The SC shows similar O:C ratios with OH exposure of $1.2*10^{11}$ molec cm^{-3} s to the those in OFR under 4.5 molec cm^{-3} s, which seems not agreeable. The different vapor losses between the SC and OFR might also a reason.

Author Response: Our OH exposures are provided as color code; hence the data requested by the referee are already presented in the main text Figure 7 and initial SI Figure S16ab. However, while all our 6 SC experiments yield a similar end-point OH exposure as the 70% UV intensity setting in the OFR (marked in organe), there are 3 SC experiments which appear to have been conducted under conditions yielding higher NO_3/OA ratios and we believe that these experiments have reached exceptionally high O/C ratios compared to the other 3 SC experiments, despite no difference in their OH exposure. To facilitate the understanding of this plot, we have prepared an additional plot of O/C ratio vs. OH exposure as suggested by the referee.

Text modifications: We have replaced our initial Figure 7 and adjusted the corresponding text.

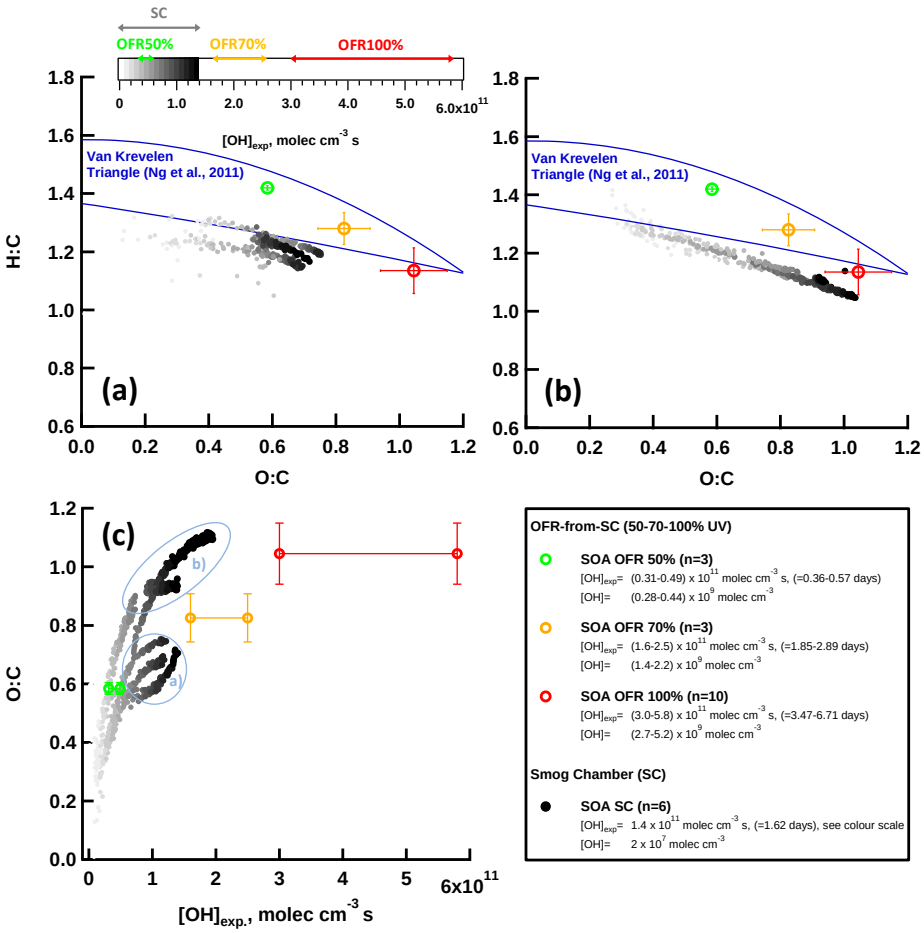

Figure R1-4: New version of Figure 7, splitting the experiments into a) and b) by their NO_3/OA ratio, as previously addressed in Figure S16 and in addition panel c) showing the plot requested by the referee (O:C vs. OH exposure); the new figure caption reads as follows:
"Bulk OA composition of SC and OFR SOA. a-b)*Van-Krevelen plot (O:C vs. H:C) for SOA formed during SC expts (n=6, GDI1 standard and w/GPF, cW and Ph 1 (cW)) and OFR-from-SC data points (n=10, GDI1 standard and w/GPF, full cW, full cE, Ph 1 (cW)) at different OFR UV settings (100%, 70%, 50%). a) shows SC Expt (A2, A3, B3; Table S4) and b)* ***SC*** *Expt (A1, B1, B2; Table S4), experiments which are characterized by a NH_4NO_3 is outside our CO_2^+-AMS interference calibration range (Pieber et al., 2016). The POA contribution was subtracted from the total OA bulk composition; SOA/POA ratios are >> 10. The Aiken parameterization (Aiken et al., 2007; Aiken et al., 2008) has been applied to HR fitted data. Lines indicate the Van-Krevelen (VK) space typical for ambient AMS measurements (Ng et al., 2011). Error bars represent one standard deviation of measurement variability.* ***(c)*** *O:C of a) and b) as a function of [OH] exposure. $[OH]_{exp}$ in days refers to an assumed average ambient [OH] of 10^6 molec cm^{-3}."*

RC1-27: Fig. 2(b) POA point is missing for GDI4-catGPF (CW)
Author Response: The data point is now visible Figure 2.
Text modifications: The revised version of Figure 2 is provided in the answer to RC-2.

RC1-28: Fig. 5 Better to show the OH exposure range as well.
Author Response: Figure 5 presents one example experiment, and the OH-exposure information is provided in the figure caption to our earlier Figure 6 and Figure 7, as already described in the initial manuscript.
Text modifications: As described in our response above, no further modifications were made.

References by RC1

See acp-2017-942-RC1 for references mentioned by Referee 1.

References to Author's Response:

Aiken, A. C., DeCarlo, P. F., and Jimenez, J. L.: Elemental analysis of organic species with electron ionization high-resolution mass spectrometry, Anal. Chem., 79, 8350-8358, 10.1021/ac071150w, 2007.

Aiken, A. C., Decarlo, P. F., Kroll, J. H., Worsnop, D. R., Huffman, J. A., Docherty, K. S., Ulbrich, I. M., Mohr, C., Kimmel, J. R., Sueper, D., Sun, Y., Zhang, Q., Trimborn, A., Northway, M., Ziemann, P. J., Canagaratna, M. R., Onasch, T. B., Alfarra, M. R., Prevot, A. S. H., Dommen, J., Duplissy, J., Metzger, A., Baltensperger, U., and Jimenez, J. L.: O/C and OM/OC ratios of primary, secondary, and ambient organic aerosols with high-resolution time-of-flight aerosol mass spectrometry, Environ. Sci. Technol., 42, 4478-4485, 10.1021/es703009q, 2008.

Barmet, P., Dommen, J., DeCarlo, P. F., Tritscher, T., Praplan, A. P., Platt, S. M., Prévôt, A. S. H., Donahue, N. M., and Baltensperger, U.: OH clock determination by proton transfer reaction mass spectrometry at an environmental chamber, Atmos. Meas. Tech., 5, 647-656, 10.5194/amt-5-647-2012, 2012.

Bruns, E. A., El Haddad, I., Keller, A., Klein, F., Kumar, N. K., Pieber, S. M., Corbin, J. C., Slowik, J. G., Brune, W. H., Baltensperger, U., and Prévôt, A. S. H.: Inter-comparison of laboratory smog chamber and flow reactor systems on organic aerosol yield and composition, Atmos. Meas. Tech., 8, 2315-2332, 10.5194/amt-8-2315-2015, 2015.

Hildebrandt, L., Donahue, N. M., and Pandis, S. N.: High formation of secondary organic aerosol from the photo-oxidation of toluene, Atmos. Chem. Phys., 9, 2973-2986, 10.5194/acp-9-2973-2009, 2009.

Jimenez, J. L., Canagaratna, M. R., Drewnick, F., Allan, J. D., Alfarra, M. R., Middlebrook, A. M., Slowik, J. G., Zhang, Q., Coe, H., Jayne, J. T., and Worsnop, D. R. (2016). Comment on "The effects of molecular weight and thermal decomposition on the sensitivity of a thermal desorption aerosol mass spectrometer", Aerosol Sci Tech. 50, i-xv, 10.1080/02786826.2016.1205728

Jordan, A., Jaksch, S., Jürschik, S., Edtbauer, A., Agarwal, B., Hanel, G., Hartungen, E., Seehauser, H., Märk, L., Sulzer, P., and Märk, T. D.: H_3O^+, NO^+ and O_2^+ as precursor ions in PTR-MS: isomeric VOC compounds and reactions with different chemical groups, 5th International Conference on Proton Transfer Reaction Mass Spectrometry and its Applications, 2011.

Krechmer, J. E., Pagonis, D., Ziemann, P. J., and Jimenez, J. L. (2016). Quantification of Gas-Wall Partitioning in Teflon Environmental Chambers Using Rapid Bursts of Low-Volatility Oxidized Species Generated in Situ, Environ Sci Technol. 50, 5757-5765, 10.1021/acs.est.6b00606

La, Y. S.; Camredon, M.; Ziemann, P. J.; Valorso, R.; Matsunaga, A.; Lannuque, V.; Lee-Taylor, J.; Hodzic, A.; Madronich, S.; Aumont, B. Impact of chamber wall loss of gaseous organic compounds on secondary organic aerosol formation: explicit modeling of SOA formation from alkane and alkene oxidation. Atmos. Chem. Phys. 2016, 16, 1417−1431.

Lambe, A. T., Ahern, A. T., Williams, L. R., Slowik, J. G., Wong, J. P. S., Abbatt, J. P. D., Brune, W. H., Ng, N. L., Wright, J. P., Croasdale, D. R., Worsnop, D. R., Davidovits, P., and Onasch, T. B.: Characterization of aerosol photooxidation flow reactors: heterogeneous oxidation, secondary organic aerosol formation and cloud condensation nuclei activity measurements, Atmos. Meas. Tech., 4, 445-461, 10.5194/amt-4-445-2011, 2011.

Middlebrook, A. M., Bahreini, R., Jimenez, J. L., and Canagaratna, M. R. (2012). Evaluation of Composition-Dependent Collection Efficiencies for the Aerodyne Aerosol Mass Spectrometer using Field Data, Aerosol Sci Tech. 46, 258-271, 10.1080/02786826.2011.620041

Murphy, D. M. (2016). The effects of molecular weight and thermal decomposition on the sensitivity of a thermal desorption aerosol mass spectrometer, Aerosol Sci Tech. 50, 118-125, 10.1080/02786826.2015.1136403

Ng, N. L., Canagaratna, M. R., Jimenez, J. L., Chhabra, P. S., Seinfeld, J. H., and Worsnop, D. R.: Changes in organic aerosol composition with aging inferred from aerosol mass spectra, Atmos. Chem. Phys., 11, 6465-6474, 10.5194/acp-11-6465-2011, 2011.

Pagonis, D., Krechmer, J. E., de Gouw, J., Jimenez, J. L., and Ziemann, P. J. (2017). Effects of gas–wall partitioning in Teflon tubing and instrumentation on time-resolved measurements of gas-phase organic compounds, Atmos. Meas. Tech. 10, 4687-4696, 10.5194/amt-10-4687-2017

Palm, B. B., Campuzano-Jost, P., Ortega, A. M., Day, D. A., Kaser, L., Jud, W., Karl, T., Hansel, A., Hunter, J. F., Cross, E. S., Kroll, J. H., Peng, Z., Brune, W. H., and Jimenez, J. L. (2016). In situ secondary organic aerosol formation from ambient pine forest air using an oxidation flow reactor, Atmos. Chem. Phys. 16, 2943-2970, 10.5194/acp-16-2943-2016

Peng, Z., Day, D. A., Ortega, A. M., Palm, B. B., Hu, W., Stark, H., Li, R., Tsigaridis, K., Brune, W. H., and Jimenez, J. L. (2016). Non-OH chemistry in oxidation flow reactors for the study of atmospheric chemistry systematically examined by modeling, Atmos. Chem. Phys. 16, 4283-4305, 10.5194/acp-16-4283-2016

Peng, Z., Day, D. A., Stark, H., Li, R., Lee-Taylor, J., Palm, B. B., Brune, W. H., and Jimenez, J. L. (2015). HOx radical chemistry in oxidation flow reactors with low-pressure mercury lamps systematically examined by modeling, Atmos. Meas. Tech. 8, 4863-4890, 10.5194/amt-8-4863-2015

Pieber, S. M., El Haddad, I., Slowik, J. G., Canagaratna, M. R., Jayne, J. T., Platt, S. M., Bozzetti, C., Daellenbach, K. R., Frohlich, R., Vlachou, A., Klein, F., Dommen, J., Miljevic, B., Jimenez, J. L., Worsnop, D. R., Baltensperger, U., and Prévôt, A. S. H.: Inorganic Salt Interference on CO_2^+ in Aerodyne AMS and ACSM Organic Aerosol Composition Studies, Environ Sci Technol, 50, 10494-10503, 10.1021/acs.est.6b01035, 2016.

Platt, S. M., El Haddad, I., Pieber, S. M., Zardini, A. A., Suarez-Bertoa, R., Clairotte, M., Daellenbach, K. R., Huang, R. J., Slowik, J. G., Hellebust, S., Temime-Roussel, B., Marchand, N., de Gouw, J., Jimenez, J. L., Hayes, P. L., Robinson, A. L., Baltensperger, U., Astorga, C., and Prévôt, A. S. H.: Gasoline cars produce more carbonaceous particulate matter than modern filter-equipped diesel cars, Sci Rep, 7, 4926, 10.1038/s41598-017-03714-9, 2017.

Turpin, B. J., and Lim, H.-J.: Species Contributions to PM2.5 Mass Concentrations: Revisiting Common Assumptions for Estimating Organic Mass, Aerosol Sci. Technol., 35, 602-610, 10.1080/02786820119445, 2001.

Weitkamp, E. A., Sage, A. M., Pierce, J. R., Donahue, N. M., and Robinson, A. L.: Organic aerosol formation from photochemical oxidation of diesel exhaust in a smog chamber, Environ. Sci. Technol., 41, 6969-6975, 10.1021/es070193r, 2007.

Zhang, X., Cappa, C. D., Jathar, S. H., McVay, R. C., Ensberg, J. J., Kleeman, M. J., and Seinfeld, J. H. (2014). Influence of vapor wall loss in laboratory chambers on yields of secondary organic aerosol, Proceedings of the National Academy of Sciences, 10.1073/pnas.1404727111

Zhao, Y., Lambe, A. T., Saleh, R., Saliba, G., and Robinson, A. L.: Secondary Organic Aerosol Production from Gasoline Vehicle Exhaust: Effects of Engine Technology, Cold Start, and Emission Certification Standard, Environ Sci Technol, 52, 1253-1261, 10.1021/acs.est.7b05045, 2018.